ITTC Quality System Manual

Recommended Procedures and Guidelines

Procedure

Seakeeping Experiments

7.5	Process Control
7.5-02	Testing and Extrapolation Methods
7.5-02-07	Loads and Responses
7.5-02-07-02	Seakeeping
7.5-02-07-02.1	Seakeeping Experiments

Disclaimer

Updated / Edited by	Approved
Seakeeping Committee of the 29th ITTC	29th ITTC 2021
Date 02/2020	Date 06/2021

Table of Contents

Seakeeping Experiments

1. PURPOSE OF PROCEDURE

This procedure outlines the recommended state-of-the-art practice of model seakeeping experiments for the evaluation of ship hull performance in predefined operational and environmental conditions.

The procedure describes requirements relevant to the selection of model size, completeness of its geometry, ballasting and mass distribution and possible model configurations. It provides recommendations for model response data measurements, and operational and environment parameters that should be included in the test plan.

The procedure also outlines the recommended approach to data analysis and presentation formats as well as the preferred approach to uncertainty analysis including theoretical background and practical examples.

2. SEAKEEPING EXPERIMENTS

2.1 Model Size

The size of the model should be such that tank wall interference is avoided for the range of wave frequencies and model speeds to be tested. Figure 1 and Table 1 give, in dimensionless form, a relationship between model length L_M, tank breadth B_T, Froude number Fr and the highest wave frequency ω at which interference effects may occur in head waves.

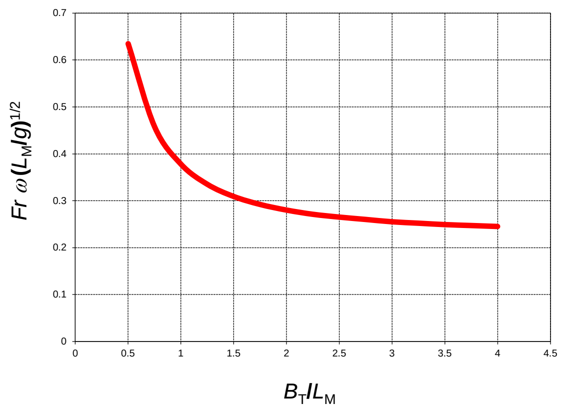

Figure 1. Maximum frequency at which tank interference occurs in head waves

Table 1. Maximum frequency at which tank interference occurs in head waves

B_T/L_M	$Fr \cdot \omega\sqrt{L_M/g}$
0.50	0.635
0.75	0.458
1.00	0.378
1.25	0.335
1.50	0.309
1.75	0.292
2.00	0.280
2.25	0.271
2.50	0.265
2.75	0.260
3.00	0.255
3.25	0.252
3.50	0.249
3.75	0.247
4.00	0.245

Those calculations are made by estimating the potential generated by a source with harmonic strength. Calculations using the unified-slender ship theory were made by Kashiwagi & Ohkusu (1991).

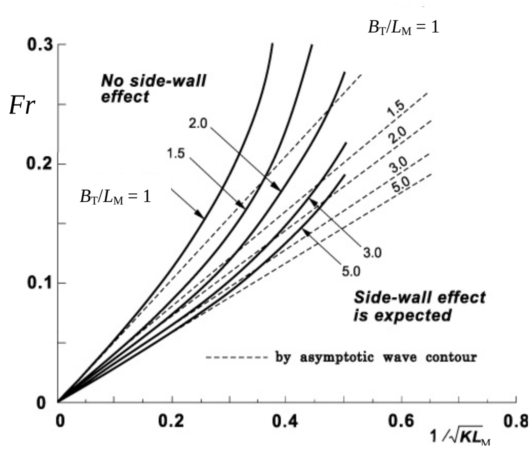

Figure 2. Estimation of tank-wall effects using unified slender theory (Kashiwagi & Ohkusu 1991).

Figure 2 shows where tank-wall effects are expected for a prolate spheroid of beam - length ratio 1/8 with $K = \omega^2/g$. The dotted lines in Figure 2 show the results of Figure 1.

Non published work of Fernandez shows that the finite depth must be taken into account in tank-wall effects for:

$$Fr \cdot \omega_e \sqrt{L_\mathrm{M}/g} \leq 1/2$$

with ω_e, the encounter circular frequency.

These estimations use calculations of the potential generated by a source with harmonic strength in finite depth. Figure 3 shows results in the same format as Figure 1.

2.2 Model Completeness

The test objectives determine the suitable level of model completeness. For many seakeeping tests, especially when undertaken for higher sea states, it is desirable that the model is complete up to the uppermost weather deck, including forecastle and bulwarks. A more complete modelling of deck fittings, deck houses and freeing ports may be necessary if parameters such as deck wetness are to be measured.

All appendages should be fitted, and the report should state which appendages were fitted during the experiments.

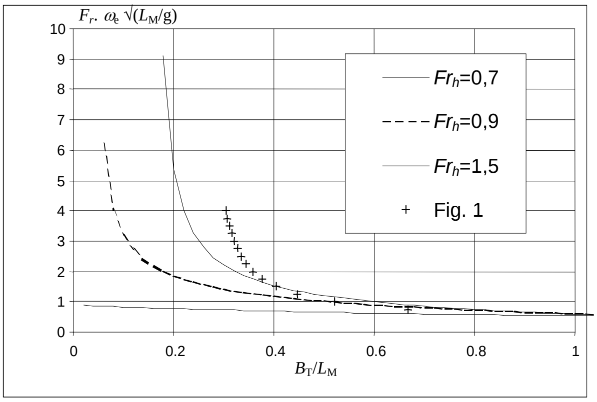

Figure 3. Maximum frequency at which tank interference occurs in head waves and finite depth.

If turbulence tripping is applied to the hull and/or the appendages of the model this should be recorded and reported for reproducibility purposes.

2.3 Model Mass Properties

2.3.1 Requirements

To achieve dynamic similarity between ship and model it is usually enough to only replicate the radii of gyration correctly for the motion directions that are not constrained during the experiments. If the longitudinal radii of gyration for pitch or yaw are unknown, a value of 0.25 L_{PP} could be used. If the transverse radius of gyration is unknown, a value between 0.35B and 0.40B, depending on the ship type, could be used. (These values are those without including the effect of added mass). Still care should be taken using these values, as some ship types are known to have deviating values and the effect on the responses can be significant (Grin and Fernandez, 2015).

For experiments during which rolling is not restrained the metacentre height should be simulated as well, besides the transverse radius of gyration. If the vertical position of the centre of gravity is unknown, it should be established and reported. As an alternative to ballasting the model to a specified transverse radius of gyration, the natural period of rolling of the full-scale ship may be simulated.

If bending moments, shears, and torsion experienced by the model in waves are to be measured, not only the radii of gyration, but also the longitudinal and transverse distributions of mass must be reproduced as correctly as possible, and must be properly reported. When measuring loads on multi hull vessels, cross products of inertia have to be taken into account. Refer to ITTC procedure 7.5-02-07-02.6 on Global Loads for more details.

2.3.2 Ballasting procedure

The model should be ballasted to the specified drafts. To allow this, draft markings for each loading condition should be present on the model on at least three stations along the length and on both port and starboard side. If practically possible the weight of the model should be measured before launching the model. This ensures that the displacement and the longitudinal centre of buoyancy (and gravity) are set correctly. If needed, adjustments in the ballast weight should be carried out until the model floats at the correct equilibrium. In case discrepancies are found in the floating equilibrium these should be reported and if possible corrected at this stage.

Next, is the check of the vertical centre of gravity. The most common way of checking this is to perform an inclination experiment. In this experiment a ballast weight is shifted over a known transverse distance on the model and the change in inclination (heeling) of the model due to the shift is measured using an inclinometer. From this the metacentre height $\overline{GM}$ can be obtained as follows:

$$\overline{GM} = \frac{p \cdot d}{\rho \nabla \cdot \tan(\Delta\phi)} \tag{1}$$

with p the weight of the shifted ballast, d the transverse distance over which the weight was shifted, $\rho\,\nabla$ the model weight, and $\Delta\varphi$ the change of model inclination (heel) angle due to the shift. Next the height of the centre of gravity $\overline{KG}$ can be obtained by:

$$\overline{GM} = \overline{KB} + \overline{BM} - \overline{KG} \tag{2}$$

The height of the centre of buoyancy $\overline{KB}$ and the metacantric radius $\overline{BM}$ can be obtained from a suitable stability software suite as are widely available in the industry for the ship geometry and loading condition(s) under consideration.

It is recommended to limit the change in model inclination to 2 to 5 degrees. Smaller heel angles would lead to possible inaccuracies in the heel angle measurement, whereas larger heeling angles may invalidate the usage of the metacentric height to approximate the stability moment. Models with a complex geometry around their floating waterline, such as highly inclined section shapes, may prohibit the usage of the initial stability to approximate their stability even at small heeling angles. For those cases use is to be made of the full curve of arms of static stability to determine the relation between heeling angle and centre of gravity.

Multiple approaches to set the radii of gyration exist. A distinction can be made between relatively simple swinging techniques, where the eigen period of the model suspended in a spring system is determined after an initial excursion and more advanced shaker techniques, where use is made of actively controlled tables often equipped with force transducers or motion measurement systems.

Some facilities make use of oscillating tables for setting the pitch and yaw radii of gyration by timing the period of oscillation. Also suspending the model from long wires fore and aft (of a specified length) and swinging the model in the horizontal plane around its centre of gravity while recording the oscillation period is a technique that is widely in use. For the pitch radius of gyration, the model would have to be suspended on its side (rotated 90 degrees around its longitudinal axis), for the yaw radius of gyration the model would be suspended straight up. Roll inertia can be determined by suspending the model in the fashion of a compound double pendulum, where the model is the “lower” limb.

More advanced techniques for establishing radii of gyration include shaker tables. A wide range of possible solutions exist in this category. Some of them are developed in-house by model testing facilities, others can be commercially bought. The most advanced arrangements place a carefully aligned model on top of a table that is supported by a multidirectional spring system and excited in arbitrary motion directions. By determining a multitude of motion modes, the apparatus is able to obtain all radii of gyration (including roll) in a single operation automatically. The springs need to be selected carefully in order to enable the accurate measurement of these motion modes.

After recording the radii of gyration, it may be necessary to shift ballast weights to obtain the specified values. Typically this is done be shifting multiple weights in opposite directions. This to avoid shifting the centre of gravity while manipulating the radii of gyration. To allow this, the model should be designed with sufficient weight margin, to allow ballast weights to be shifted. As shown by Liu & Papanikolaou (2017) relatively small deviations from the desired pitch gyradius can have a significant influence on added resistance in waves.

Finally, the roll natural period follows from the transverse metacentre height and the transverse radius of gyration and can be checked in the water by performing an decay test with the model freely floating. After giving the model an initial excursion, the natural roll period can be obtained by recording the roll period of the motion. It is recommended to average the roll period over multiple roll oscillations, for typical applications 10 oscillations is practical. To match the roll period measured in water with the ‘dry’ roll radius of gyration the added mass in roll should be taken into account. Preliminary calculations with simple potential flow based software tools (such as 2-dimensional strip theory) can be used to obtain reasonable estimation of the added mass in roll.

In cases where the dry roll radius of gyration is unknown but the natural roll period is specified, an alternative approach can be to set the roll natural period directly by performing roll decay tests and shifting ballast weights until the desired period is reached.

In many cases an iterative approach is necessary to set the condition the model, with a final check on the floating equilibrium with the draft markings, an inclination test to check the metacentric height, and decay tests to check the roll (and in some cases the pitch) periods.

It is recommended to repeat these checks during the course of a testing campaigns, as the weight distribution properties of a model may change over time due to (unforeseen) equipment and model changes and due to the fact that models may absorb certain quantities of water over time, depending on the material used and their coating.

2.4 Guidance System

The guidance system should be such as to impose the minimum restraint on the motions of the model. It is desirable that even in head or following waves the model should have the freedom to roll. In oblique waves, care also must be taken to minimize restraint on sway and yaw motions.

The report should describe in detail the characteristics of the guidance system used. Should the guidance system be a soft mooring arrangement with springs, the natural frequency of the system for each heading should be far from the wave frequency range. The recommended ratio of natural mooring frequency to wave (peak) frequency is 1/6.

Model control systems used in seakeeping experiments, particularly with respect to autopilot and roll stabilization, usually serve two objectives:

- to assess the sea-keeping capabilities of a vessel in a reliable and repeatable manner, and/or,
- to assess the efficacy of a full-scale design for a particular control system or set of control surfaces.

The approach taken in the first one is to replace the need for a human pilot in sea-keeping experiments. Automatic control eliminates differences seen in sea-keeping experiments caused by differences in operation between human pilots. Care must be taken, however, to ensure that the control system dynamics of the automatic steering do not interfere with the vessel dynamics being measured in a seaway in an unrealistic fashion.

The second item above applies to scenarios in which a full-scale control design is to be evaluated. In this case, care must be taken to ensure that the dynamics of the full-scale control system are preserved. Note that such control systems will likely influence the open-loop dynamics of the vessel and impact the vessel's natural sea-keeping performance.

In Appendix B of this document and in the 28th ITTC Proceedings, more details are given for the theory behind the tuning procedures for control systems in model scale particularly for heading control, tracking control, roll stabilization through active fins and roll stabilization through rudder. High-level tuning procedures themselves (for both seakeeping experiments as well as scaled control assessment experiments) are detailed.

2.5 Free Running Tests

Testing with a free running self-propelled model is the preferred method for seakeeping experiments. Experiments are usually run at predefined speeds. Preliminary tests can be necessary to adjust the rpm in order to reach the desired speed in waves. Alternatively, the rpm can be automatically controlled to obtain the desired mean speed in waves.

The autopilot parameters should be chosen to reflect a realistic full-scale response of the model. Care should be taken in selecting a realistic rudder rate during model tests. These parameters should be reported.

Care has to be taken to reduce any influence of cables or safety lines on the model's motions to a minimum.

It is recommended that rpm and rudder action are continuously recorded.

2.6 Measurement of Wave Loads

Segmented models for measuring global loads should have natural frequencies far from the wave frequency range to ensure that the model structural responses do not affect the measured loads. These frequencies have to be measured and documented. For more details, refer to ITTC recommended procedure 7.5-02-07-02.6 on global loads seakeeping experiments that discusses also elastic (segmented) models.

The mass, CG and inertias of each separate segment have to be known (measured or calculated) and reported. Preferably, the loads due to the mass and inertia of the segments should be separated from the total loads during analysis to get the wave-induced loads. In any case this has to be reported in case the local mass distribution per segment (mass, CG and inertia) does not match that of the full scale vessel. For the global bending moment, both sagging and hogging loads should be reported.

2.7 Power increase in waves

The power increase in waves can be measured directly with free running models or determined indirectly from measurements of added resistance. The results of these tests are input for determining the power increase in a seaway as described in ITTC recommended procedure 7.5-02-07-02.2 and the weather factor f_w for decrease of ship speed in waves as described in ITTC recommended procedure 7.5-02-07-02.8.

Usually, added resistance (or power increase) in waves is measured in the process of basic seakeeping tests, along with motions and motion related effects. Thus, general recommendations outlined in this procedure for seakeeping experiment are also valid for added resistance tests.

Below a number of different approaches are described that can be used to generate the values required by the analysis as described in ITTC recommended procedure 7.5-02-07-02.2.

2.7.1 Added resistance test in regular waves

The experimental estimation of the added resistance in waves is performed in two steps:

the measurement of the (mean) still water resistance, R_{SW}, at speeds of interest,
the measurement of the (mean) total resistance in waves, R_{T}, at same speeds.

These two measurements give values of the resistance force averaged over the run time. Added resistance is obtained as a difference between the two measured mean values:

$$R_{\mathrm{AW}} = R_{\mathrm{T}} - R_{\mathrm{SW}} \quad (3)$$

Runs in still water and in waves should be preferably performed using one and the same model at one and the same loading condition and the same model setup. The model should be equipped with all appendages, fixed rudder and propeller hub, but without propeller. If relative motions are to be measured the relative wave probes should be installed during still water tests as well, under the assumption that they do not create additional force in waves. However, in specific cases of multiple probes or massive holders, their influence on added resistance should be specially addressed by duplicate testing with and without probes.

Two methods of towing could be applied:

a) constant thrust (model free to surge),
b) constant speed (surge restricted).

It has been shown by Journee (1976) that both methods give compatible results for added resistance and do not influence motion measurements. The application of specific towing techniques thus depends on the towing apparatus that is available.

In principle, the constant thrust method gives more freedom to model motions and results in less oscillations of the instantaneous resistance force about its average, but it requires a more complicated design of the towing apparatus, including for instance a constant tension winch or linear motor to provide the constant thrust. For oblique sea cases both setups can be challenging, as now also roll motions should be allowed by the test setup, while the towed setup needs to deal with heading and or course keeping.

The constant speed method is easy to implement as a conventional semi-captive setup can be used. In head waves the model should be able to heave and pitch, in oblique seas roll motions should be considered as well. A disadvantage of the constant speed method is that it results in large oscillations of the resistance force and eventual loss of accuracy at instant overshooting of force gauge limits, especially in high waves. One way of offsetting this is to use a clamp setup that unloads the resistance force transducer during the model acceleration and deceleration phases of the test. This allows the selection of more sensitive (and fragile) force transducers to measure the resistance.

Measurement of added resistance in regular waves does not require larger samples than these in case of regular seakeeping (motion) experiments and is thus performed within one test run at least a similar number of encounters as is given for regular waves (10, refer to section 2.11) in general is sufficient, provided that the motions and added resistance have reached steady state. In some cases taking more encounters (20 to 25) is prudent to ensure convergence of the added resistance.

2.7.2 Self-propulsion test in regular waves

Analogously to 2.7.1, the procedure consists of two sets of runs, as follows:

a) estimation of self-propulsion point in terms of RPM, torque, thrust or power in still water at certain speed,
b) estimation of corresponding self-propulsion point in waves.

Then the increase in propulsive characteristics (added RPM, added torque, added thrust or power increase) are obtained as a difference between average values measured in still water and in waves.

Principles for model preparation correspond to those outlined in 2.7.1, but drive engine and propeller are installed in addition. If the model is free-sailing, then the rudders should be made actively steerable and controllable.

Two techniques for model guidance are commonly applied:

a) captive model (model connected to carriage by a force gauge, zero force corresponds to the self-propulsion point). Several runs at various RPM are to be performed to get the self-propulsion point at any speed of interest, speed being controlled by the towing carriage,
b) free-running (auto-piloted and speed controlled) model. Several runs at various RPM are to be performed to get the self-

propulsion point at any speed of interest, the average speed being controlled by a tracking system.

It should be noted that both methods are an sufficient accurate approximation of the real ship operational condition, where both RPM and speed vary even slightly within one wave period (i.e. Grande et. Al (1992)). In principle it is possible to mimic the effect of the full scale engine under a varying load by special controllers. The effect on the accuracy of the test is expected to be minor, and should be weighed against the additional complication of the experimental set-up.

A possible disadvantage of using a free-sailing model is the introduction of an interpolation error over the speed when matching the results as function of speed between the calm water runs and the runs in waves. It is difficult to ensure that both tests are performed at the exact same (mean) speed.

The selection of the target self-propulsion point regime depends on the adopted method for the power prediction in waves as described in ITTC recommended procedure 7.5-02-07-02.2. In the case of modelling at the ship Self-Propulsion Point (SPP), the additional force to account for skin-friction effects must be applied both in still water and in waves, assuming that that the average friction per wave period remains equal to the friction in still water. This force is assumed to be steady and can be applied by weights or, more correctly, by using a fan installed on the model. In a similar way, other steady forces, like wind forces on the superstructure, can be modelled.

To determine the SPP at each ship speed of advance, around three to four successive runs at various RPM settings are usually required. In case of a captive model the transition time is shorter and measurement could be completed within a single run. The transition time (the time required to reach steady state after the start of the test run) for free-running models is larger and it may take more runs until a steady motion regime is reached.

2.7.3 Tests in irregular waves

There is no practical difference in performing resistance tests or self-propulsion tests in regular or irregular seas, except for the time duration of the experiments. It is common practice to collect resistance data in parallel with seakeeping (motions) tests. The required number of wave encounters to obtain convergence of statistics as recommended for general irregular seakeeping tests is discussed elsewhere in this procedure. Considering added resistance (power) as a second-order force, however, some resent studies (i.e. Naito & Kihara (1993) and Kim & Kim, (2010)) arrived at a time span of 1 to 1.5 hours (real full scale time duration) necessary to ensure convergence of resistance estimates. Repetitive runs in different time-domain realisations (‘seeds’) of the same wave spectrum are normally conducted to accumulate the required full scale run duration.

2.8 Measurement of Impact Loads

The guidelines for the measurement of impact loads are presented in procedure 7.5-02-07-02.3 Loads and Responses Seakeeping, Experiments on Rarely Occurring Events.

2.9 Parameters to be Measured

The capability to measure the following additional parameters should be provided:

Hull motions, motion rates and/or accelerations in the desired degrees of freedom.

(Incident) wave height with a probe mounted close to the model, but not causing interference. The probe should preferably be fixed to the carriage, but measurements may be made at a fixed point in the tank. In the latter case, the measuring point should be selected in the position where waves are fully formed without being affected by the waves reflected at the wave maker and the tank walls & beaches.

Relative motion/relative wave elevation. Measurements of the relative motion between the model and the water surface at points that allow correlation with wave and other motion data. Non-contact probes are preferable for wave measurements moving with the model, especially at high speeds. There are reliable wave tape sensors available that are flush with the hull at a specific station and cause no interference. Alternatively, such sensors can also be considered.

Rudder angle. In cases where active rudder control is employed, the rudder control signal and actual rudder angle should be continuously monitored.

Impact pressures on the hull or on deck at selected locations.

Still water resistance and added resistance in waves (if not freely running).

Water on deck.

Propeller revolutions. Whenever a self-propelled model is used, the shaft revolutions should be recorded.

Visual records. Tests should be recorded by video, preferably in a way allowing scaling of time.

Additionally, the following parameters may be measured depending on the test requirements:

Propeller torque and thrust be also continuously recorded.

Encounter (heading) angle. The angle between the mean model heading and the wave direction.

Leeway (or drift) angle. The angle between the mean model heading and the tangent to the path of *CG*.

2.10 Headings

When performing tests in oblique seas, the range of encounter angles between zero and 180 degrees should be selected in accordance with the stated test objectives. The 180 degrees heading represents head seas.

2.11 Regular Waves

For conventional ship forms, a sufficient number of tests should be carried out at each speed to provide adequate data for a minimum range of wave lengths from at least 0.5 L_{PP} to 2.0 L_{PP}. More tests with closely spaced wave lengths can be necessary to ensure a good definition in the resonance region. Depending on the test requirements and wave making capabilities, either the ratio of the wave height to L_{PP} or the ratio of wave height to wave length should be maintained constant. When maintaining a constant ration, the recommended value of the ratio of wave height to wave length is around 1/50 when only linear responses are of interest.

For new or unconventional hull forms and to investigate inception of large or extreme responses (around resonance frequencies, parametric roll) experiments in wave frequencies equivalent to a wavelength of 4.0 L_{PP} or higher should be considered. For similar reasons wave height to wavelength ratios of 1/30 to 1/20 or less, depending on model facilities limits should be taken into account.

It should be noted that wave steepness has a large influence on the quality and (non)linearity of the generated waves and the resulting model responses. In case of the waves being generated containing nonlinear effects this may also affect the definition of wave amplitude and wave height and therefore by extension the definition of the non-dimensionalized responses (in the form of Response Amplitude Operators – RAOs). Therefore, it should be clearly documented how the wave and response amplitudes have been obtained when reporting RAO values.

In determining the motions, it is recommended that the average amplitude and period of at least 10 cycles be obtained. Alternatively, a spectral analysis following the procedures for irregular waves outlined below could be followed to obtain the mean amplitude and period of waves and responses. Guidelines for regular wave data analysis are given in the ITTC Recommended Procedure 7.5-02-07-03.2 "Analysis Procedure for Model Tests in Regular Waves".

2.12 Transient Waves

The transient wave technique is an experimental technique in which a wave train that contains wave components of all the relevant frequencies is produced in such a way that the component waves reach a certain place in the test tank simultaneously so that a single large wave packet is formed. If a model structure is positioned at the place where the single large wave packet accumulates, response characteristics to regular waves of all the frequencies contained in the wave packet are obtained in one single experiment (provided the linear superposition assumption holds).

This technique proves to be very efficient as a standard tool for evaluating RAO's of stationary offshore structures or towed/self-propelled ships. Due to the short time duration of the wave packet possible reflections in the testing basin are avoided. Clauss (1999) gives an overview of the technique and its application to seakeeping tests for evaluating RAOs and its application the simulation of design storm waves.

A related technique to efficiently obtain the linear response characteristics is the use of a broad banded spectrum of a specific shape to obtain RAOs. A typical spectrum used for this application is pink noise (ITTC, 2002).

2.13 Irregular Waves

Tests should be carried out in waves corresponding to the sea conditions in which the vessel may be required to operate. In the absence of specific wave spectrum data the ITTC spectrum should be used for open ocean and JONSWAP spectrum should be used for fetch-limited seas. When generating irregular waves in a tank, the input signal to the wave maker should be produced such that the generated waves are not repeated within the generated wave train.

Irregular wave generation in experimental tanks is subjected to voluntary or involuntary truncation of idealized spectrum as a result of mechanical limits of wave making facilities. The truncation frequency is facility specific and depends on the characteristics of the wave maker and the model scale selected for the experiment. Selection of a too low cut-off frequency affects the properties of the resultant wave spectrum and the values of the target significant wave height $H_{W1/3}$ and modal period T_P. If $n=f_T/f_P$ with f_T the truncated frequency and f_P the spectral peak frequency of idealized wave spectra, the recommended ratio n for cut-off frequency for most facilities is greater than 2, and preferably approaching 3. For very large model scales this may not always be feasible and the amount of wave energy lost by truncating the wave spectrum should be considered carefully. Additionally, if the wave spectrum causes significant wave breaking this will also modify the spectrum significantly and may lead to a desire to modify the spectrum to avoid this breaking (Kent & Lee, 2016).

Data should preferably be digitised before analysis, using sample rates appropriate for the avoidance of aliasing with the individual measured parameters. Care must be taken for the duration of the data acquisition so that enough data are recorded for the objective of the test.

The test duration is represented by the total number of wave encounters *N*. *N*=50 should be taken as a lower limit. Larger values are to be preferred and it is more usual to take *N*=100 as the standard; *N*=200 or above is considered excellent practice. For the following sea case, 30 minutes of equivalent full scale is considered sufficient.

The time interval between test runs is also important and can be tank specific. A residuary tank disturbance of less than 1% of the next target wave height is recommended. In most cases 20 minutes between runs will be acceptable for a typical facility. For wider tanks and tanks equipped with beaches along the long side of the tank the waiting time may be shorter.

The sample rate in the data acquisition needs to be fast enough in order to achieve sufficient resolution. A sampling rate corresponding to about 4 Hz at full scale is more or less the minimum for most measurements, although typically higher values are used, for instance 100 Hz at model scale. Much higher rates (in the order of kHz) are necessary to detect and accurately capture peaks of slamming loads.

Energy spectra of waves and relevant responses should be produced through spectral analysis using either the indirect method of Fourier transformation of the autocorrelation function, or the direct method of splitting the record into suitable blocks and subjecting these to a Fast Fourier Transform. A comparison of the spectrum of the generated waves with the target spectrum should be carried out, since resulting vessel responses may be sensitive to particular parts of the spectrum (ITTC, 2002). Note that there is significant random process uncertainty on this calculation of the observed spectrum (Kent & Lee, 2016).

In addition to the spectral analysis, statistical analysis should be performed to produce at least the mean, maximum, minimum, and the mean of 1/3 highest values. In the presentation of the results the techniques utilised to smoothen spectral shapes, such as block overlapping, should be documented. When reporting statistics, the number of events and number of encounters should also be reported together with the overall statistics.

When non-linear effects and extremes are of importance, attention should be paid to more detailed wave characteristics (ITTC, 2002) and the response characteristics. Considering the probability distributions of the wave elevation and the individual crest and troughs as well as the probability distributions of the individual peaks in the response can be helpful in this respect.

For the measurement and analysis of rarely occurring events such as slamming or wetness refer to ITTC recommended procedure 7.5-02-07-02.3.

2.14 Pre-simulations

In irregular wave testing in cases where the conditions of interest are not pre-defined, a simulation tool should be used to select relevant conditions. The selection of the modal period, wave height and wave spectral shape can significantly affect the results due to both interaction with the natural periods of the model, basin limitations and other factors. 2D strip theory calculations are generally sufficient to identify regions where the motions of interest occur, but if the model motion are shown to be large and nonlinear then further consideration is needed. If available, a simulation with non-linear wave damping being modelled may be used.

Similar to irregular wave testing, for regular wave testing simulations can serve to provide guidance as to which amplitude and frequencies excite motions of interest in the model for a given speed and heading. This can enable a more streamlined test matrix for some types of testing.

2.15 Data Presentation

The coordinate system in which data are presented should be defined and reported. Motion components should also be defined. Linear translations and rotations may be presented in non-dimensional form as being divided by wave elevation and wave slope respectively.

Translations	$\frac{x_{1,2,3}}{\varsigma_A}$
Rotations	$\frac{x_{4,5,6}}{\kappa\varsigma_A}$

Dimensional presentations can sometimes be more appropriate depending on the objectives of the experiment. Phase angles should be given in degrees and increases in resistance and propulsion parameters should be presented in the non-dimensional form. Accelerations should be made non-dimensional by $L_{\mathrm{PP}}/(g\zeta_{\mathrm{A}})$. It is recommended that the results are plotted to a base of $\omega\,(L_{\mathrm{PP}}/g)^{1/2}$or $\omega_{\mathrm{e}}(L_{\mathrm{PP}}/g)^{1/2}$, although, depending on the objectives of the experiment, other bases such as wave-length - ship length ratio or wavelength may be appropriate. The limit of tank wall interference effects should be indicated on the plots.

For tests in irregular waves, the corresponding wave-energy spectrum should be defined. Preferably both the target spectrum and the actually realized spectrum should be reported.

When appropriate, performance in irregular waves should be presented in non-dimensional form involving a characteristic wave period or frequency and a characteristic wave height.

The results of statistical analyses may be presented to depict probability of exceedance and as cumulative probability distribution for selected responses.

Tabular presentation of results is recommended in addition to plots.

3. PARAMETERS

3.1 Parameters to be Considered

The following parameters defining the tests are to be taken into account (as applicable):

Scale
Model dimensions
Ratios of model to tank dimensions
Hull configuration (lines, appendages, superstructures, ...)
Loading conditions (displacement and draft)
Mass distribution (CG, inertias, ...)
Towing and/or restraining device characteristics (specially DOF)
Speeds and headings

Wave characteristics (heights, periods, spectra, dispersions, ...)
Autopilot control law and gains
Speed control characteristics
Run duration
Number of runs per test condition
Positions of sensors (accelerometers, relative motion, encountered wave, ...)
Resonance frequencies for segmented models
Sampling frequency
Sensor calibrations and accuracy

3.2 Recommendations of ITTC for Parameters

1975 Performance in irregular waves should be presented in non-dimensional form involving wave characteristic period and characteristic wave height.

1978 Recommendation for open ocean spectral formulation:

$$S(\omega; H_{W1/3}, T) = \frac{A_S}{\omega^5} e^{-\frac{B_S}{\omega^4}} \quad (4)$$

where:

$$A_S = 173 H_{W1/3}^2 / T_1^4 \approx \frac{H_{W1/3}}{4\pi}\left(\frac{2\pi}{T_2}\right)^4$$
$$B_S = 691/T_1^4 \approx \frac{1}{\pi}\left(\frac{2\pi}{T_2}\right)^4 \quad (5)$$

with the significant wave height $H_{W1/3}$ and the spectral peak period T_0, the average period T_1 and the average zero crossing period T2 and their approximate relations:

$$T_1 = 2\pi m_0/m_1$$
$$T_2 = 2\pi\sqrt{m_0/m_2} \quad (6)$$
$$T_0 \approx 1.296 T_1 \approx 1.408 T_2$$

and the spectral moments m_n given as:

$$m_n = \int_0^\infty \omega^n S(\omega) d\omega \quad (5)$$

1984 Recommendation for long crested limited fetch sea spectral formulation:

$$S(\omega; H_{W1/3}, T_1) = 155 \frac{H_{W1/3}^2}{T_1^4 \omega^5} \exp\left(-\frac{944}{T_1^4 \omega^4}\right) 3.3^\gamma \quad (6)$$

where:

$$\gamma = \exp\left[-\frac{(0.191\omega T_1 - 1)^2}{2\sigma^2}\right]$$
$$\sigma = \begin{cases} 0.07 & \omega < 5.24/T_1 \\ 0.09 & \omega > 5.24/T_1 \end{cases} \quad (7)$$

This formulation can be used with other characteristic periods by use of the following approximate relations:

$$T_1 \approx 0.924 T_{-1} \approx 0.834 T_0 \approx 1.073 T_2$$

where T_{-1} is the energy average period ($2\pi m_{-1}/m_0$), $T_0$is the spectral peak period, T_1 is the average period ($2\pi m_0/m_1$) and $T_2$is the average zero crossing period estimated from the spectrum ($2\pi\sqrt{m_0/m_2}$).

In case of short-crested seas the directional spectrum *E* can be composed by combining the frequency spectrum *S* with an angular distribution (directional spreading) function *D* (see also ITTC guideline 7.5-02-07-01.1):

$$E(\omega; H_{W1/3}, T, \alpha, \theta) = S(\omega; H_{W1/3}, T) D(\alpha, \theta)$$

$$D(\alpha, \theta) = \begin{cases} \frac{2^{2s-1}}{\pi} \frac{\Gamma^2(s+1)}{\Gamma(2s+1)} \cos^{2s}\left(\frac{\theta-\alpha}{2}\right) & \text{for } |\theta - \alpha| \le \pi \\ 0 & \text{otherwise} \end{cases} \quad (8)$$

with *s* the directional spreading parameter (a positive integer) and *Γ* the Gamma function. Superposition can be used to handle the case of two directional sea conditions, e.g. sea and swell with different directions and significant wave heights.

4. VALIDATION

4.1 Uncertainty Analysis

The detailed procedure of uncertainty analysis following the principles behind the ISO-GUM is shown in the Appendix A.

4.2 Benchmark Tests

1) Seagoing Quality of Ships. (7th ITTC, 1955, pp.247-293). A model of the Todd-Forest Series 60 with C_B=0.60. Results from 7 tanks are presented.
   Fr = 0, 0.18 ,0.21 ,0.24 ,0.27 and 0.30
   L_{PP}/H = 36, 48, 60, 72
   $\lambda/{}_{pp}$= 0.75, 1.0, 1.25, 1.5

2) Comparative Tests at Three Experimental Establishments with the Same Model. (11th ITTC, 1966, pp.332-342)
   British Towing Tank Panel: A 10 ft. Fibreglass model of the S.S. Cairndhu.
   A series of experiments on a ship model in regular waves using different test techniques.
   Data obtained in irregular and transient waves and some result predicted by the theory (based on Korvin Kroukovsky's work and employing the added mass and damping coefficients calculated by Grim).

3) Full Scale Destroyer Motion Tests in Head Seas (11th ITTC, l966, pp.342-350).
   Comparison among motion responses obtained from full scale tests, model experiments and computer calculations for destroyer H.M. "Groningen" of the Royal Netherlands Navy

4) Experiments in Head Seas For Series 60.

4-1) Comparative Tests of a Series 60 Ship Model in Regular Waves (11th ITTC, 1966, pp.411-415). Series 60 with C_B=0.60.

4-2) Experiments on Heaving and Pitching Motions of a Ship Model in Regular Longitudinal Waves (11th ITTC, 1966, pp.415-418). Series 60 with C_B=0.60.

4-3) Experiments on the Series 60 with C_B=0.60 and 0.70 Ship Models in Regular Head Waves (11th ITTC, 1966, pp.418-420)

4-4) Comparison of Measured Ship Motions and Thrust Increase of Series 60 Ship Models in Regular Head Waves (11th ITTC, 1966, pp. 420-426).

4-5) Estimation of Ship Behaviour at Sea from Limited Observation (11th ITTC, 1966, pp.426-428)

5) Analysis of the S-175 Comparative Study (17th ITTC, 1984, pp.503-511).

6) S-175 Comparative Model Experiments (18th ITTC, 1987, pp.415-427)

7) Rare Events (19th ITTC, 1990, pp.434-442). Comparison of results from tests at 12 establishments in irregular waves. Absolute and relative motions. S-175 at $Fr = 0.275$.

8) The ITTC Database of Seakeeping Experiments (20th ITTC,1993, pp.449-451).

8-1) Tests of Two Dimensional Models. Added mass, damping and wave exciting forces

8-2) Tests of a Wigley hull form. Added masses, damping, exciting forces and seakeeping motions and loads.

8-3) Tests for S-175.

9) The ITTC Database of Seakeeping Experiments (21st ITTC, 1996, pp.43). S-175, high speed marine vehicle

10) Numerical and Experimental Investigation to Evaluate Wave-Induced Global Design Loads for Fast Ships (Schellin et al, 2003). Two segmented models of fast ships (*Fr* up to 0.63) were tested in head seas. Motions and global loads are reported. The results are compared with several non-linear codes.

5. REFERENCES

Clauss, G.F., 1999, "Task-related wave groups for seakeeping tests or simulation of design storm waves", Applied Ocean Research, vol. 21, pp. 219-234.

Gerhardt, F.C., Kjellberg, M., 2020, "A comparison of experimental and numerical seakeeping results for the KVLCC2 tanker". Paper in preparation, publication early 2020.

Grin, R. And Fernandez Ruano, S., 2015, "On the prediction of radii of inertia and their effect on seakeeping", Proceedings of the 12th International Marine Design Conference, pp. 189-203.

ISO/IEC 2008, "Guide 98-3, Uncertainty of measurements – Part 3: Guide to the expression of uncertainty in measurements (GUM: 1995)", 2008 Switzerland.

ITTC, 2002, "The Specialist Committee on Waves – Final Report and Recommendations to the 23rd ITTC", Proceedings of the 23rd International Towing Tank Conference, vol. 2, pp. 505-736.

ITTC, 2008, "Discussion to the 25th ITTC Seakeeping Committee by Joe Longo, Claus Simonsen, Fred Stern", Proceedings of 25th International Towing Tank Conference, vol. 3, Fukuoka, Japan.

Kashiwagi, N. and Ohkusu, M., 1991, "A new theory for side-wall interference effects on forward-speed radiation and diffraction forces", Schiffstechnik, vol. 38.

Kent, C.P. and Lee, S.-S., (2016), "Wave-Breaking Modification and Spectral Statistics of Wave Spectra", Proceedings of 31st Symposium on Naval Hydrodynamics, Monterey, CA, USA.

Kishev, R., (1998), "Uncertainty Analysis of Dynamic Model tests and Its Application to Capsizing Simulation in Waves", Proceedings of the International Workshop on Modeling of Ocean Environments in Waves & Current Basin, February, 1998, Taejon, Korea.

Liu, S., & Papanikolaou, A., (2019). "Approximation of the added resistance of ships with small draft or in ballast condition by empirical formula", Proceedings of the Institution of Mechanical Engineers, Part M: Journal of Engineering for the Maritime Environment, 233(1), 27–40.

Schellin, T.E. et al, 2003, "Numerical and Experimental Investigation to Evaluate Wave-Induced Global Design Loads for Fast Ships", Transactions SNAME, vol. 111, pp. 437-461.

Yum, D.J., Lee, H.Y. and Lee, C.M., 1993. "Uncertainty Analysis for Seakeeping Model Tests", Journal of the Society of Naval Architects of Korea, 30 (3): 75-89.

Appendix A.

A.1. Background to ISO-GUM

The recommendation of the ITTC 2008 was to adopt the ISO-GUM (International Organization for Standardization, Guide to the Expression of Uncertainty in Measurements, ISO 1995) approach to conducting uncertainty analysis of experimental results. The ISO GUM recognises two groups of uncertainty, type A and type B, which are based on way in which the uncertainty is evaluated. Type A represents the random category of uncertainty evaluated by using statistical analysis of repeated measurements of, nominally, the same observation; type B components are estimated by means other than repeated observations. The “other means” may include previous measurements, past experience or general knowledge, handbook information, manufacturer specification or data provided as a certificate. A detailed approach to uncertainty analysis in experimental hydrodynamics can be found in ITTC procedure 7.5-02-01-01.

A.1.1. Type A uncertainty

The fundamental form of uncertainty associated with a measurement is type A, $u_A(x_i)$, which can be expressed as a standard deviation. Type A uncertainty is typically based upon the analysis of repeated measurements which characterizes the randomness of the experimental process. The most common approach to estimating type A uncertainty is by undertaking end-to-end multiple repeated runs; care should be taken to ensure that as many factors as possible that affect repeatability of experiment are accounted for. Numbers of repeats should be as large as practicable in order to minimize type A uncertainty; however 10 repeats indicates good experimental practice. However, in most seakeeping tests it is not practicable to carry out multiple repeats for all experimental conditions. It may be more feasible to select only characteristic or unique test conditions (due to environment and/or operations) for which repeat runs should be undertaken and reported. Historic database of information on Type A uncertainty could be created (occasionally confirmed) and used to report uncertainty for routine experiments.

A.1.2. Type B uncertainty

Type B uncertainty, $\mathrm{u_B}(x_i)$, may be considered as an approximation to the experimental variance or standard deviation respectively. In the same way as type A uncertainty, type B is assumed to be equal to the standard deviation $u_S(x_i)$. Typically type B uncertainty can be estimated from quoted values of uncertainty, assumed statistical distribution of the parameters and factors depending on a level of confidence in the measurement. Generally, the experimenter can assume that the type B uncertainty is normally distributed around some mean, however, in some specific cases is may be pertinent to consider alternatives such as triangular or rectangular distributions. For type B uncertainty that is assumed to be normally distributed Table A1 shows the factors that need to be applied for some examples of confidence.

Table A1. Confidence factors for normally distributed type B uncertainties

Confidence Level [%]	Factor
50	0.6757
68.27	1.
90	1.645
95	1.96
99	2.576
99.73	3

For example, this means that, statistically, one can have 95% confidence that a measurement lies within a value of $\pm 1.96\mathrm{u}(\mathrm{x_i})$.

A.1.3. Standard uncertainty

The standard uncertainty, $u_S(x_i)$, in a measured value is the summation of type A and all of the type B uncertainties and can be calculated using the uncertainty propagation formula:

$$\mathrm{u_S}(\mathrm{x_i}) = \left(\sum_{i=1}^{N} \mathrm{u_A}^2(\mathrm{x_i}) + \sum_{j=1}^{K} \mathrm{u_B^2}(x_i)\right)^{\frac{1}{2}} \quad \text{(A1)}$$

A.1.4. Combined uncertainty

A further step is required when result of an experiment is derived from values of a number of other measurement variables (x_i). The most common situation where this is undertaken in seakeeping experiments is when the results are non-dimensionalised. In this case, the combined uncertainty $u_C(y)$ is applied to express uncertainty in the derived result.

$$u_C(\mathrm{y}) = \left(\begin{array}{l}\sum_{i=1}^{N}\left(\frac{\partial \mathrm{f}}{\partial \mathrm{x_i}}\right)^2 \mathrm{u_S}^2(\mathrm{x_i}) + \\ +2\sum_{i=1}^{N-1}\sum_{j=i+1}^{N}\frac{\partial \mathrm{f}}{\partial \mathrm{x_i}}\frac{\partial \mathrm{f}}{\partial \mathrm{x_j}}\mathrm{u_S}(\mathrm{x_i},\mathrm{x_j}\end{array}\right)^{\frac{1}{2}} \quad \text{(A2)}$$

The second term in the combined uncertainty formula represents the cross correlation between two or more variables. These terms are zero when variables are considered to be independent. The $\frac{\partial f}{\partial x_i}$ term is the partial derivative with respect to variable x_i, also known as the sensitivity coefficient and $u_S(x_i)$ is the standard uncertainty of variable x_i.

A.1.5. Expanded uncertainty

When presenting the results of experiments along with interval expressing some level of confidence in that measurement then the expanded uncertainty U is applied.

$$U = ku_C(y) \quad \text{(A3)}$$

where, k represents the confidence or coverage factor, and the result of the measurement can be interpreted as $y\text{-}U \leq Y \leq y+U$.

So, Y can be interpreted as the best estimate that the resultant measurement lies within the range $y\text{-}U$ and $y+U$; the value of U is defined by k. For cases where the uncertainty can be assumed to be normally distributed the confidence factors presented in Table 1 can be used. For example, a value k=2.576 value gives confidence level of 99%.

A.2. Sources of uncertainty

A typical requirement from a seakeeping experiment is to obtain the basic rigid body motions (surge, sway, heave, roll, pitch and yaw), accelerations and relative motions at specific locations, waves, model speed, and propulsion and steering systems characteristics (propeller revolutions, rudder angle). All of these measured parameters are subjected to type A and type B uncertainties that need to be estimated as a part of the experimentation procedure.

A.2.1. Type A uncertainty

As indicated in section A.1.1 type A uncertainty is evaluated by taking repeated measurements of the same experimental condition (recommended number of repeated runs is 10). Since repeating the entire set of test runs in a seakeeping experiment makes the programme prohibitively long (and hence expensive) it is recommended that only a few selected representative test conditions should be repeated to obtain some understanding of the type A uncertainty.

A.2.2. Type B uncertainty

There are elemental type B uncertainties that are an inherent part of each sensor, its calibration, the data acquisition system, processing and analysis.

All of these elemental type B uncertainties should be accounted for, using in equation A2, to determine the type B uncertainty for each measured parameter.

A.2.2.1. Sensors

Measurements of the rigid body motions of the model, accelerations and relative motions, propulsion and control parameters are usually primary requirements of seakeeping experiments. Specifications provided by the manufacturers of the sensors used in experiments, coupled with past experience in the use of such sensors, allows an estimation of the relevant type B uncertainty to be made. The manufacturer may present sensor uncertainty information as standard deviations (or multiples of) or as an expanded uncertainty with a specified confidence level. This information can be translated to a standard deviation and can be used to obtain the standard type B uncertainty for that particular element. For example, a sensor specification stating that roll and pitch angles are measured to a dynamic accuracy of 0.5 degrees rms can be interpreted as a 0.5 degree standard uncertainty in roll and pitch. In most cases individual sources of uncertainty need to be identified from available specification documents and the uncertainty propagation formula should be used to obtain the standard uncertainty given in (A1).

Elemental sources of uncertainty that are usually identified from manufacturer's specification may include: non-linearity, hysteresis, non-repeatability, zero offset drift, spam temperature coefficient, and resolution.

A.2.2.2. Calibrations

Before used in experiments, all instruments need to be calibrated; either bench or in-situ calibration or else factory calibration constants are applied.

Calibration characterises an instrument's uncertainty but does not eliminate it; indeed, the calibration process itself is subject to uncertainties. Generally, a system level, in-situ end-to-end calibration is advisable that includes as many of the possible elemental sources of uncertainty in the calibration procedure. A few, additional, elemental sources of uncertainty need to be considered when estimating uncertainty: calibration standards (quality of calibration specimens or injection source), calibration curve fitting, calibration set up (misalignments) and A/D conversion.

The uncertainty associated with the quality of the calibration standard and calibration device/jig set-up misalignments can be estimated from the manufacturer's specification. Uncertainty due to calibration standards B_{CS} can be estimated using:

$$u_{\text{BCS}} = \sqrt{\sum (A_{\text{CG}} \cdot W_i)^2} \tag{A4}$$

A_{CG} accuracy of calibration specimens; e.g., weight, distance, angle…

W_i physical values of calibration points; weight, distance, angle…

The uncertainty associated with misalignment in the calibration set-up u_{BCM} can be evaluated from:

$$u_{\text{BCM}} = \sum (W(1 - \cos\alpha_j) \tag{A5}$$

W nominal measurement value
α angle of misalignment in relevant plane.

The curve fitting uncertainty can be estimated using the standard error of estimation (SEE) formula:

$$\mathrm{SEE} = \left[\frac{1}{n(n-1)}\sum_1^n\left(\mathrm{y_n} - \mathrm{y_{LS,k}}\right)^2\right]^{1/2} \qquad \text{(A6)}$$

In the formula n is the number of calibration samples, y_n is calibration data point, and $y_{LS,n}$ is fitted value. In most cases n ≥ 7 is recommended. It can be assumed that the SEE value is approximately equal to the standard uncertainty.

Generally, the majority of data acquisition systems that are currently in use employ a 16-bit (or better) analogue to digital (A/D) converters. However, some specific equipment may still use 12-bit A/Ds to acquire model data.

The type B uncertainty associated with the A/D conversion u_{BCAD} is equivalent to ½ the resultant resolution and can be estimated from:

$$u_{BCAD} = \frac{1}{2}\frac{TotalVoltageRange}{A/Dbits} \cdot CalibrationFactor \qquad \text{(A7)}$$

The *TotalVoltageRange* is typically equal to either ±10 Volts or ±5 Volts; the *A/Dbits* value is 2^{16} or 2^{12} for 16 and 12 bit convertors respectively, the *CalibrationFactor* is a calibration constant that translates voltage to physical units. Typically, uncertainty due to resolution of 16-bit system would be negligible, but for 12-bit system it could be significant for higher precision instrument.

In the case of measuring instruments that are provided with manufacturer calibration data (most modern digital instruments) calibration standards are reflecting standards of high precision source (voltage) that, normally, is expected to be considerably more accurate than accuracy that can be achieved in a physical bench calibration.

It is advisable, if practical, to conduct in-situ end-to-end (with all model systems being active) calibration of the sensors that are to be used in the experiment. In such a situation, the calibration process should include all or most elemental type B uncertainty sources, which are difficult to estimate individually. However, for in-situ calibration they don't have to be individually identified and estimated.

This approach does not exclude the need for uncertainty analyses due to calibration standards, set up, curve fitting and other related sources of uncertainty but hopefully overall simplifies the procedure.

A.2.2.3. Data Acquisition System.

In case when in-situ end-to-end calibration procedure is applied all data acquisition system elemental error sources are included in the process except for noise due to variation in surrounding external environment (temperature, humidly) and other used devices (propulsion motor). Good testing practice requires screening of all noise sources, but when this appears to be difficult those effects should be estimated.

A.2.2.4. Data processing.

Type B uncertainty due to data reduction and analysis should include any uncertainty related to data integration, differentiation, filtering and other methods of data manipulation. It can be evaluated based on previous experience of working with data processing systems. Uncertainty due to any data reduction associated with the calculation of basic statistics (mean, standard deviation) should be considered negligible, however, for more complex data manipulations resultant uncertainty may need to be considered. These uncertainties can be estimated by using the same data manipulation process with a known signal with known analytical solution (sin or cosine) comparing the processed and analytic outputs.

A.2.2.5. Data analysis.

Model speed and heading. - Model speed uncertainty is subjected to both type A and type B uncertainties. The type A component is calculated using equation for the standard uncertainty (the uncertainty propagation formulae A1) and the combined uncertainty (A2). The Type B uncertainty component is dependent upon the method in which the model speed is obtained. If, during the experiments, the model is attached to or follows the carriage and speed of the model can be assumed to be equal to the speed of the carriage, then the method presented in ITTC 2008 7.5-02.07-02.1 and that suggested by Fogash (1992) can be used.

Under the assumption that model speed, v, through the water is equal to the speed of towing carriage, the model speed is determined from

$$v = \frac{n/5000\pi D}{t} = \frac{f\pi D}{5000} \quad \text{(A8)}$$

where D(m) is the diameter of carriage wheel and $n$is the number of light pulses sensed by the photo coupler during the time period t. The 5000 number is facility specific and indicates number of pulses per single turn of carriage wheel. The measured quantities and error sources for the estimation of model speed and error limit are the diameter of carriage wheel and the pulse frequency $f(=n/t)$.

The combined uncertainty becomes, in this case:

$$u_C(\mathrm{v}) = \left[\left(\frac{\partial \mathrm{v}}{\partial f}\right)^2 u^2(f) + \left(\frac{\partial \mathrm{v}}{\partial D}\right)^2 u^2(D)\right]^{\frac{1}{2}} \quad \text{(A9)}$$

$$u_C(\mathrm{v}) = \begin{bmatrix} \left(\frac{\pi D}{5000}\right)^2 \mathrm{u}^2(f) + \ldots \\ \ldots \left(\frac{\pi f}{5000}\right)^2 u^2(D) \end{bmatrix}^{\frac{1}{2}} \quad \text{(A10)}$$

If a free running model is used in the experiments and, for example, an optical tracking system is used for to determine model position, then v=*s/t* should be applied, and the instantaneous and/or mean speed can be calculated (*s* is distance between two consecutive sampled positions, and *t* is time between two consecutive samples). In this case, the combined uncertainty formula can be used to obtain model speed uncertainty:

$$u_C(v) = \left[\left(\frac{\partial v}{\partial s}\right)^2 u^2(s) + \left(\frac{\partial v}{\partial \mathrm{t}}\right)^2 u^2(t)\right]^{\frac{1}{2}} \quad \text{(A11)}$$

$$u_C(v) = \left[\left(\frac{1}{t}\right)^2 u^2(s) + \left(-\frac{s}{t^2}\right)^2 u^2(t)\right]^{\frac{1}{2}} \quad \text{(A12)}$$

Standard (or combined) uncertainties $u(s)$ and $u(t)$ need to be estimated based on information provided on model positions and accuracy of sample time. Nominal values of *s* and *t* should be applied to obtain combined uncertainty.

Similarly, if a captive model is used or free running model follows the carriage the heading angle is assumed to be equal to the heading of the carriage with respect to the oncoming waves. For free running, self-propelled models when an optical system is used to obtain model positions the instantaneous (and mean) heading angle can be estimated from consecutive longitudinal and lateral positions of the model. The estimate of combined uncertainty in heading is then based on the uncertainty in the lateral and longitudinal position of the previous and next location of the model, and the nominal longitudinal and lateral distance between those two points. The arctangent is applied to estimate the uncertainty in the angle based on the uncertainty in the ratio of the lateral (ΔY) and longitudinal (ΔX) consecutive positions. Uncertainty in the ratio can be calculated from:

$$u(\frac{\Delta Y}{\Delta X}) = \begin{bmatrix} \left(\frac{\partial\left(\frac{\Delta Y}{\Delta X}\right)}{\partial(\Delta Y)}\right)^2 u^2(\Delta Y) + \\ + \left(\frac{\partial\left(\frac{\Delta Y}{\Delta X}\right)}{\partial(\Delta X)}\right)^2 u^2(\Delta X) \end{bmatrix}^{\frac{1}{2}} \qquad \text{(A13)}$$

$$u(\frac{\Delta Y}{\Delta X}) = \begin{bmatrix} \left(\frac{1}{\Delta X}\right)^2 u^2(\Delta Y) + \\ + \left(-\frac{\Delta Y}{(\Delta X)^2}\right)^2 u^2(\Delta X) \end{bmatrix}^{\frac{1}{2}} \qquad \text{(A14)}$$

Nominal ΔX and ΔY values are calculated from the mean heading angle, and the appropriate uncertainty can be used to calculate uncertainty in the ratio.

In case when model heading is obtained after double integration of yaw rate measurement, both uncertainty of yaw rate measurement and accuracy of integration procedure need to be included in combined uncertainty estimate.

Model geometry and mass distribution - sources of uncertainty in model geometry are model length (L_{PP}), width (B) and draft (T). For seakeeping experiments the position of centre of gravity ($\overline{KG}$) and longitudinal radius of gyration (k_{yy}) are also important and their respective uncertainties need to be determined.

Typical suggested tolerances on the principal parameters associated with model geometry are +/-0.05% on linear dimensions larger than 2m, and +/-1mm on dimensions less than 2 m, and +/-1% on model displacement. In all cases they are the type B uncertainties that are constant for the duration of experiment. Examples of achieved and/or suggested uncertainties of model main parameters and mass properties as well as presented results are shown in Kishev (1998) and ITTC (2008).

Uncertainties in model geometry can be determined using past experience in model construction. For instance, if a model manufacturer states that a 5-metre long model is accurate to within +/-2.5 mm with 90% confidence, then one can assume that the expanded uncertainty of the model length is +/-2.5 mm. The standard uncertainty can be estimated, using the confidence factor in Table 1, from expression 2.5/1.645=1.52 assuming that a normal distribution can be applied to represent the stated value. So, the resultant standard uncertainty of the length is ~1.5 mm.

To estimate the uncertainty in the model $\overline{KG}$ and k_{yy},, the propagation of uncertainty needs to be applied to the formula used to calculate these respective values. For example if $\overline{KG}$ of a model is estimated based on inclining experiments and the following formula is employed: $\overline{KG} = \overline{KB} + \overline{BM} - \overline{GM}$. The vertical centre of buoyancy ($\overline{KB}$) and transverse metacenter ($\overline{BM}$) are geometry dependent, when metacentric height ($\overline{GM}$) can be obtained from inclining experiment. The combined uncertainty in $\overline{KG}$ can be evaluated from:

$$u_C(\overline{KG}) = \begin{bmatrix} \left(\frac{\partial\overline{KG}}{\partial\overline{KB}}\right)^2 u^2(\overline{KB}) + \\ + \left(\frac{\partial\overline{KG}}{\partial\overline{BM}}\right)^2 u^2(\overline{BM}) + \\ + \left(\frac{\partial\overline{KG}}{\partial\overline{GM}}\right)^2 u^2(\overline{GM}) \end{bmatrix}^{\frac{1}{2}} \qquad \text{(A15)}$$

The standard uncertainty of $\overline{GM}$ can be estimated by applying combined uncertainty formula to:

$$\overline{GM} = \frac{w \cdot d}{W \cdot \tan(\varphi)} \quad \text{(A16)}$$

where, w is inclining weight, d is distance the inclining weight is moved, W model displacement, φ is heel angle when inclined.

The combined uncertainty of $\overline{GM}$ can be presented as:

$$u_C(\overline{GM}) = \begin{bmatrix} \left(\frac{\partial \overline{GM}}{\partial w}\right)^2 u^2(w) + \\ + \left(\frac{\partial \overline{GM}}{\partial d}\right)^2 u^2(d) + \\ + \left(\frac{\partial \overline{GM}}{\partial W}\right)^2 u^2(W) + \\ + \left(\frac{\partial \overline{GM}}{\partial \varphi}\right)^2 u^2(\varphi) \end{bmatrix}^{\frac{1}{2}} \quad \text{(A17)}$$

$$u_C(\overline{GM}) = \begin{bmatrix} \left(\frac{d}{W \cdot tg\varphi}\right)^2 u^2(w) + \\ + \left(\frac{w}{W \cdot tg\varphi}\right)^2 u^2(d) + \\ + \left(-\frac{w \cdot d}{W^2 tg\varphi}\right)^2 u^2(W) + \\ + \left(-\frac{w \cdot d}{W \cdot \sin^2\varphi}\right)^2 u^2(\varphi) \end{bmatrix}^{\frac{1}{2}} \quad \text{(A18)}$$

Standard uncertainty of $\overline{KB}$ and $\overline{BM}$ can be evaluated by assuming a simplified geometry of hull form and using known standard uncertainties of main parameters.

For example, the transverse $\overline{BM}$ for a triangle-prism shaped vessel with a rectangular water plane area can be calculated from:

$$\overline{BM} = \frac{I}{V} = \frac{LB^3}{12\nabla} = \frac{LB^3}{12 \cdot \frac{1}{2} LBT} = \frac{B^2}{6T} \quad \text{(A19)}$$

Where, I is second moment of rectangular water plane area about its centreline, ∇ volume of displacement, and L, B and T are length and breadth of water plane respectively and T is draft of the vessel.

The combined uncertainty of $\overline{BM}$ is:

$$u_C(\overline{BM}) = \begin{bmatrix} \left(\frac{\partial \overline{BM}}{\partial B}\right)^2 u^2(B) + \\ + \left(\frac{\partial \overline{BM}}{\partial T}\right)^2 u^2(T) \end{bmatrix}^{\frac{1}{2}} \quad \text{(A20)}$$

$$u_C(\overline{BM}) = \begin{bmatrix} \left(\frac{B}{3T}\right)^2 u^2(B) + \\ - \left(\frac{B^2}{6T^2}\right)^2 u^2(T) \end{bmatrix}^{\frac{1}{2}} \quad \text{(A21)}$$

Nominal B and T values, and their respective uncertainties need to be applied to calculate combined uncertainty in transverse $\overline{BM}$.

A similar procedure can be used to evaluate the combined uncertainty in the vertical location of centre of gravity and longitudinal radius of gyration k_{yy} that could be obtained a pendulum experiment.

Wave parameters – the uncertainty in wave measurements (regular and irregular) is one of major sources of uncertainty in experiments. Limitations of wave generators, the deterioration of wave properties propagating forward of experimental facilities and reflections from beach devices contribute to uncertainty in the wave environmental. Those uncertainties are difficult to estimate and are usually neglected. Target irregular wave properties are normally defined as significant wave height, modal period and type of spectrum. Additionally, there is significant uncertainty due to random process uncertainty (Kent &Lee, 2016) that is not addressed here.

Target regular wave properties are described by wave amplitude and frequency. Wave matching is normally conducted based on a measurement in one selected-representative location, and supported by measurements in a few other locations to check for consistency. Two sources of error for which uncertainty could be estimated are difference between the target and matched wave(s) and uncertainty due to measuring and processing errors.

Either regular or irregular wave properties are generally obtained from measurements of wave displacement using devices such as a sonic wave probe and/or capacitance wave probes. Basic statistics from measurements provide rms that can be used as a first estimate of the amplitude of regular waves ($\zeta_A = \sqrt{2} \cdot rms$) and significant height of irregular waves ($H_{W1/3} = 4 \cdot rms$). Spectral analysis can be also be employed to determine significant height of irregular waves $H_{W1/3} = 4\sqrt{m_0}$, where m_0 is area under the energy spectrum curve.

Total standard uncertainty in wave amplitude or height measurements should be evaluated using the uncertainty propagation formula. Type A uncertainty can be evaluated from repeated observations for different wave seeds or approaches (Kent & Lee, 2016), although this can be impracticable for seakeeping experiments, and type B uncertainty established from properties of measuring device and data process.

Wave direction is also a significant parameter when undertaking experiments in oblique waves. Verification of waves propagation direction can be carried out using many instruments. One possible choice for the validation of wave direction with respect to the tank could be by using a 3D acoustic Doppler velocimeter. Periodic repeated wave measurements for selected wave directions can be carried out to determine standard deviation and standard uncertainty. The direction can be verified during wave matching for a specific experiment.

A.2.2.6. Data presentation

It is customary to present the final experimental results in a standardized format - usually non-dimensionalised. The linear translations from regular waves tests are typically non-dimensionalised by wave amplitude; rotations by wave slope and amplitude, and accelerations by $L_{PP}/(g \cdot \zeta_A)$. Generally these non-dimensional responses are presented to a base of the non-dimensional encounter wave frequency given as $\omega_e\sqrt{L_{PP}/g}$

Therefore, the combined uncertainty u_c of the non-dimensional heave displacement $z' = z/\zeta_A$ can be calculated from the following:

$$u_C(z') = \begin{bmatrix} \left(\frac{\partial z'}{\partial z}\right)^2 u^2(z) + \ldots \\ \ldots \left(\frac{\partial z'}{\partial \zeta_A}\right)^2 u^2(\zeta_A) \end{bmatrix}^{1/2} \quad \text{(A22)}$$

$$u_C(z') = \begin{bmatrix} \left(\frac{1}{\zeta_A}\right)^2 u^2(z) + \ldots \\ \ldots \left(-\frac{z}{\zeta_A^2}\right)^2 u^2(\zeta_A) \end{bmatrix}^{1/2} \quad \text{(A23)}$$

Where, z and ζ_A are heave displacement and regular wave amplitude, $u(z)$ and $u(\zeta_A)$ are respective total standard uncertainties of measured heave displacement and wave amplitude including all type A and type B elemental error sources.

Similarly, combined uncertainty of non-dimensional encounter frequency $\omega_e' = \omega_e\sqrt{L_{PP}/g}$ can be evaluated from:

$$u_C(\omega_e') = \begin{bmatrix} \left(\frac{\omega_e'}{\omega_e}\right)^2 u^2(\omega_e) + \ldots \\ \ldots \left(\frac{\omega_e'}{L_{PP}}\right)^2 u^2(L_{PP}) \end{bmatrix}^{1/2} \quad (A24)$$

$$u_C(\omega_e') = \begin{bmatrix} \left(\frac{L_{PP}}{g}\right) u^2(\omega_e) + \\ + \left(-\frac{\omega_e}{2(L_{PP} \cdot g)^{1/2}}\right)^2 u^2(L_{PP}) \end{bmatrix}^{1/2} \quad (A25)$$

Again, ω_e, L_{PP} and g are respective nominal values, and $u(\omega_e)$ and $u(L_{PP})$ are respective standard uncertainties.

Motions in irregular seas are typically presented as plots of non-dimensional or significant values versus velocity, Froude number or sea state.

For example, formulae for non-dimensional pitch motion and the resulting combined uncertainty are as follow:

$$C_\theta = \frac{\theta \cdot L_{pp}}{2\pi \cdot H_{W1/3}} \quad (A26)$$

$$u_C(c_\theta) = \begin{bmatrix} \left(\frac{\partial C_\theta}{\partial \theta}\right)^2 u^2(\theta) + \\ + \left(\frac{\partial C_\theta}{\partial H_{W1/3}}\right)^2 u^2(H_{W1/3}) + \\ + \left(\frac{\partial C_\vartheta}{\partial L_{PP}}\right)^2 u^2(L_{PP}) \end{bmatrix}^{\frac{1}{2}}$$

where:

$$\frac{\partial C_\theta}{\partial \theta} = \frac{L_{PP}}{2\pi \cdot H_{W1/3}}$$

$$\frac{\partial C_\theta}{\partial H_{W1/3}} = -\frac{\theta L_{PP}}{2\pi \cdot H_{W1/3}^2}$$

$$\frac{\partial C_\theta}{\partial L_{pp}} = \frac{\theta}{2\pi \cdot H_{W1/3}}$$

θ is the significant pitch angle response in irregular wave.

Combined uncertainty in estimation of Froude number ($Fr = V/\sqrt{gL_{PP}}$) can be expressed as follow:

$$u_C(Fr) = \sqrt{\begin{matrix} \left(\frac{\partial Fr}{\partial V}\right)^2 u^2(V) + \ldots \\ \ldots \left(\frac{\partial Fr}{\partial L_{PP}}\right)^2 u^2(L_{PP}) \end{matrix}} \quad (A27)$$

where,

$$\frac{\partial Fr}{\partial V} = \frac{1}{\sqrt{gL_{PP}}}$$

$$\frac{\partial Fr}{\partial L_{PP}} = -\frac{V}{2\sqrt{gL_{PP}^3}}$$

Once the experimental data have been collected and reduced to non-dimensional format for a particular wave encounter frequency and/or Froude number, they can be presented in a tabular format or we may want to obtain a mathematical expression to represent the data. In this case regression can be performed on the experimental data (after data reduction) and a polynomial equation fit to represent the data. The type B uncertainty associated with the regression should be included in the analysis.

A.2.3. Example

Table A2 and Figure A1 present examples of total standard and combined uncertainty calculations of model parameters and responses from submarine model seakeeping surface experiments in irregular seas.

From the table one can conclude that the uncertainty in the model main parameter is contained below 1%, and that the type B uncertainty is dominating model motions measurements.

A.2.4. Summary

The above presented procedure outlines ITTC recommended ISO GUM approach to uncertainty analysis in seakeeping experiment measurements. Intention of the procedure is to emphasize details unique for seakeeping experiment measurements and data presentation. Background information for ISO GUM approach and assumptions are discussed in ITTC Specialists Committee on Uncertainty Analysis procedure 7.5-02-01-01. The methodologies presented here are relevant to uncertainties in measurements only. Subject of uncertainty in predictions is not included in the above discussions.

Table A2. Estimate of uncertainty for responses during seakeeping experiments

Source of uncertainty	Nominal Value	Units	Description of accuracy	Type A uncertainty	Type B uncertainty	Standard uncertainty
Model Lpp	4.70	m	+/- 3 mm, 90% confidence		0.0018	0.002
Model B	0.51	m	+/- 2 mm, 90% confidence		0.0012	0.001
Model T	0.52	m	+/- 2 mm, 90% confidence		0.0012	0.001
Model D	671.14	m^3	resultant		0.0042	0.004
Model KB	0.29	m	resultant		0.0012	0.001
Model BM	0.302	m	resultant		0.0004	0.000
Model KG	0.264	m	inclining experiment		0.0015	0.002
Model kxx	0.213	m	swing frame		0.0024	0.002
Model GMt	0.038	m	resultant		0.0008	0.001
Speed 1	3.4	knots	Optical tracking Qualisys	0.057	0.012	0.059
Speed 2	6.2	knots	Optical tracking Qualisys	0.042	0.016	0.063
Speed 3	12.9	knots	Optical tracking Qualisys	0.052	0.028	0.108
Roll Angle 1	13.8	deg	FOG	0.190	2	2.009
Roll Angle 2	17.5	deg	FOG	0.169	2	2.007
Roll Angle 3	1.7	deg	FOG	0.054	2	2.001
Pitch Angle 1	3.5	deg	FOG	0.063	2	2.001
Pitch Angle 2	1.1	deg	FOG	0.028	2	2.000
Pitch Angle 3	0.7	deg	FOG	0.041	2	2.000
Heave Displ. 1	2.12	m	Motion Pack	0.030		0.030
Heave Displ. 2	2.14	m	Motion Pack	0.020		0.020
Heave Displ. 3	0.38	m	Motion Pack	0.017		0.017
Vert. Accel. 1	0.16	g	Honeywell, QA 1400	0.001	0.0031	0.003
Vert. Accel. 2	0.14	g	Honeywell, QA 1401	0.002	0.0031	0.004
Vert. Accel. 3	0.04	g	Honeywell, QA 1402	0.001	0.0031	0.003
Relative Mot. 1	1.33	m	ULS, USS 635	0.018	0.0013	0.018
Relative Mot. 2	1.43	m	ULS, USS 635	0.008	0.0013	0.008
Relative Mot. 3	0.69	m	ULS, USS 635	0.010	0.0013	0.010
Wave Elev. 1	2.62	m	Capacitance probe	0.004	0.004	0.005
Wave Elev. 2	1.84	m	Capacitance probe	0.005	0.004	0.007
Wave Elev. 3	0.64	m	Capacitance probe	0.006	0.004	0.007
						Combined Uncertainty
Froude no. 1	0.07					0.0022
Froude no. 2	0.12					0.0024
Froude no. 3	0.25					0.0041

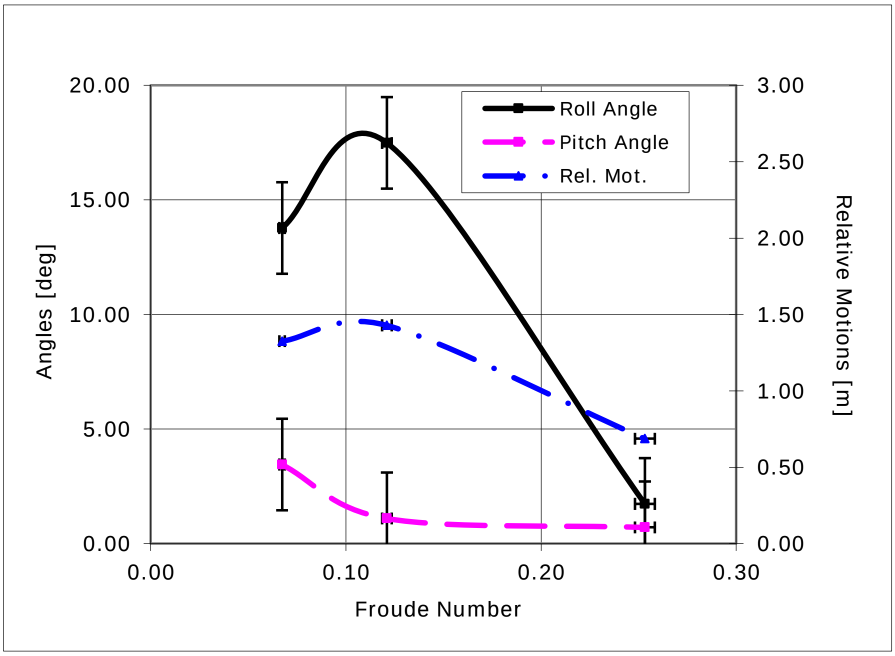

Figure A1. Example of responses and range of uncertainty

Appendix B.

B.1. Model control systems tuning

The following outlines the tuning of steering controllers and roll stabilizers using PD / PID-based tunings for standard monohull displacement-hull vessels with a single rudder control surface (or multiple rudder surfaces controlled together). In this process it is assumed that either

All lifting surfaces are modelled using Froude scaling

Or model scale deflection forces are functionally mapped to full-scale deflection forces.

Note that the tuning method outlined here is for a defined forward speed. For each forward speed, the process must be re-iterated to capture the vessel dynamics at that speed.

B.2. Heading control through steering

B.2.1. Background

Heading control through steering is based on the Nomoto first-order steering model which relates rudder as an input to yaw rate (Fossen, 1994).

The first order Nomoto steering model is given by:

$$\frac{\dot{\psi}}{\delta}(s) = \frac{K_N}{(1 + T_N s)}$$

Where $\dot{\psi}$ is yaw rate, δ is the rudder angle K_N is the static yaw rate gain, T_N is time constant and s is the complex variable of the Laplace transform.

To determine the model parameters, execute a standard “zig-zag” manoeuvre (or any large rudder angle to large yaw angle manoeuvre).

The resulting data set can be used to identify model parameters by either system identification methods or graphical methods using a response plot. It should be noted that an identified Nomoto parameter pair is valid for one forward speed only. As an example, for a Mariner Class vessel K_N and T_N are given as 0.185 and 107.3 in (Fossen, 1994).

The form of this approximation for the steering dynamics contains a single pole, which defines the system's steering bandwidth. In the above approach, the yaw rate is related to the rudder angle. Whereas in practice the aim is to control the heading angle, ψ, and not the time derivative of ψ. Therefore, an integrator to the transfer function models needs to be added. With the integrator, there will be two poles in the system. Hence, when a state feedback control is applied, the goal is to move the two poles of the closed loop system into a complex conjugate pair to produce damped, harmonic response. Overshooting is the result of an under-damped system. Also, an over-damped response, where the damping ratio, ζ, is greater than one, is generally not desirable.

In designing a controller, the bandwidth is chosen so that the inherent natural frequency of the vessel is not altered. This way, the model's natural behaviour is not interfered by the control system performance.

The details of the underlying theory for the above discussions can be found in the 28th ITTC Proceedings. A solution satisfying the above mentioned considerations for the controller can be given as follows:

$$k_P = \omega_0^2 T_N / K_N$$

$$k_D = \frac{2\zeta\omega_0 T_N - 1}{K_N}$$

where k_p is proportional gain, k_d is derivative gain, T_N and K_N are as described above, ω_0 is equivalent natural frequency and $\zeta$is damping ratio as mentioned above.

B.2.2. Guidelines for the heading controller design

The steering controller is recommended to be designed as follows:

1. Identify Nomoto model parameters as outlined above for each forward speed.
2. Best-fit the parameters to the linearized Nomoto model using established procedures developed to fit these parameters from zig-zag data. If possible, system identification techniques may be used, reducing the need for "ideal" zig-zag information. (If a prohibitive number of forward speeds are to be tested - such that determining the Nomoto for each speed is practically very difficult – a range of parameters can be estimated including parameters for the minimum and maximum forward speeds, and two or three speeds in between.)
3. Choose, through pole placement techniques, the desired PD or PID tuning for the autopilot.
4. A different tuning will be utilized for each forward speed to preserve the open-loop characteristics. The following procedure is developed for first-order Nomoto approximations and a PD state feedback control system:

A damping ratio ζ is selected based on the desired response. For each calibrated forward speed K_N and T_N parameters will be identified, which also define the system bandwidth and natural frequency ω_0. Given these parameters, proportional gain k_P and derivative gain k_D can be calculated using the equations given above. Integral gain can be conservatively added if it is deemed necessary to eliminate offset.

The gains calculated using this method provide a useful starting point for tuning steering controllers with minimum influence on seakeeping response.

B.3. Track control

Simple autopilot-based track controllers typically function by providing a heading trajectory signal into the input of the autopilot heading controller. There are numerous methods available to generate a suitable path-tracking trajectory.

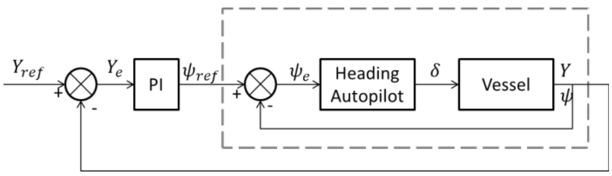

Figure B1. A simple heading autopilot (dashed box) with a simple PI "sway-keeping" outer loop.

Track control is typically implemented in basin seakeeping experiments for the purpose of reducing sway drift-off or "crabbing" events, i.e., to follow a straight path over ground. When used for seakeeping experiments, care must be taken to ensure that any trajectory fed into the autopilot controller does not alter the dynamics of that controller itself.

A simple straight path tracking control scheme can be seen in Figure B1. In this simple case, an outer PI control loop is used to generate the reference signal for the simple heading autopilot to hold a track (with a global Y set-point). When tuning this controller, the overall bandwidth of the control scheme must follow the open-loop bandwidth of the vessel. Conservatively tuning the outer PI loop to control with slower dynamics than the autopilot inner-loop will suffice to ensure that the vessel can track without influencing seakeeping.

More complicated track controllers and trajectory-generating schemes are not recommended for seakeeping experiments, but may be implemented for other test purposes. Examples of these may be found in "Handbook of marine craft hydrodynamics and motion control" by Thor Fossen and other references.

B.4. Roll motion reduction

B.4.1. Active fin stabilization

Fin stabilization systems are highly effective for roll damping. Using lift generated on these surfaces at speed, fins can provide correcting moments which oppose that of the vessel's roll, thus increasing damping. Fin dynamics do not couple significantly into other axes (assuming that they are placed appropriately near midships) and should not require special control considerations to preserve vessel dynamics. Fin rates must be capable of performing a full fin angle sweep in a roll period to be effective.

The simplest control scheme for a fin stabilizer is to feed the roll rate signal (with proportional gain term) into the fin deflection controller.

B.4.2. Rudder roll stabilization (RRS)

Typically used in conjunction with an autopilot, RRS Systems use high-frequency rudder motions to stabilize a vessel in roll by adding roll damping to a ship. Before modeling this type of controller, the following considerations must be made:

A significant bandwidth separation must exist between the steering-yaw subsystem and the steering-roll subsystem, that is, the frequencies of effective roll subsystem cannot be low enough to affect the low-frequency bandwidth of the steering subsystem. This will cause degradation in the performance of both controllers.

The steering gear must be capable of withstanding high frequency motions (both model-scale and full-scale), on the order of the roll frequency. Steering systems are typically designed for low-frequency motions under high loads, and hydraulic pump systems typically have lower duty-cycles, unless specifically designed for RRS. The maximum steering gear slew rate must be:

$$\dot{\alpha}_{max} \geq \omega_{\phi}\alpha_{max}$$

where α is rudder angle correction and ω_{ϕ} is natural roll frequency.

Natural roll frequency / damping must be characterized through the speed envelope of the vessel.

Unlike the seakeeping autopilot, use of active roll stabilization systems in a test-basin setting tests the performance of the roll stabilizer controller itself, and as such, care must be taken to appropriately scale the controller properties to predict full-scale performance.

B.4.2.1. Guidelines for the rudder roll stabilization (RRS)

Design choices made in the scaling of lift surfaces and propellers may induce issues when attempting to model full-scale controllers in model-scale. For autopilot control and stabilization control, dynamic response is predicated mainly upon scaling the full-scale moments (and machinery slew rates) appropriately.

Modelling full-scale rudders and fins is a difficult trade-off: modelling them with the appropriate geometry scaling can result in lift curves that vary from that of the full-scale design curves. Modelling them with the correct Froude lift-scaling can result in different sizes and areas, affecting efficiency, resistance, and flow. Whichever design choices are taken to model the lift surfaces, two important aspects must be considered to achieve the appropriate model-scale response:

Forces (and thus, moments) applied must be appropriately scaled, and,

Time to generate these forces (generally, “slew rates”) must be scaled.

Care must be taken on the implementation of the second point: it is not sufficient to scale the machinery rates in time if the lift curves are not scaled appropriately. From a control perspective, it is not the lift surface angle that has to be achieved/limited in a span of time (i.e., a machinery slew rate), but rather the lift force (a force slew rate).

This can be achieved through a functional mapping, that is,

Full-Scale Angle » Full-Scale Force » Model-Scale Force » Model-Scale Angle

and,

Full-Scale Slew Rate » Full-Scale Force Rate » Model-Scale Force Rate » Model-Scale Slew Rate

Control gains are also scaled via Froude scaling laws.

B.5. References

Fossen, T., 1994, “Guidance and control of ocean vehicles”, John Wiley & Sons Inc.

Fossen, T., 2011, “Handbook of marine craft hydrodynamics and motion control”, John Wiley & Sons, Ltd.

Kent, C.P. and Lee, S.-S., (2016), "Wave-Breaking Modification and Spectral Statistics of Wave Spectra", Proceedings of 31st Symposium on Naval Hydrodynamics, Monterey, CA, USA.

Ogata, K., 2001, "Modern control engineering", Prentice Hall PTR.

Perez, T., 2005, "Ship motion control", Springer-Verlag London Ltd.